NUCLEAR SCIENCE AND TECHNIQUES **25**, 030601 (2014)

Numerical analysis of pressure load in a PWR cavity in an ex-vessel steam explosion*

ZHONG Ming-Jun (钟明君),[1] LI Zhi-Gang (李志刚),[1] LIN Meng (林萌),[1]
HUANG Xi (黄熙),[1] ZHOU Yuan (周源),[1,†] and YANG Yan-Hua (杨燕华)[1]

[1] *School of Nuclear Science and Engineering, Shanghai Jiaotong University, Shanghai 200240, China*
(Received August 12, 2013; accepted in revised form March 22, 2014; published online June 20, 2014)

Ex-vessel steam explosion may happen as a result of melting core falling into the reactor cavity after failure of the reactor vessel and interaction with the coolant in the cavity pool. It can cause the formation of shock waves and production of missiles that may endanger surrounding structures. Ex-vessel steam explosion energetics is affected strongly by three dimensional (3D) structure geometry and initial conditions. Ex-vessel steam explosions in a typical pressurized water reactor cavity are analyzed with the code MC3D, which is developed for simulating fuel-coolant interactions. The reactor cavity with a venting tunnel is modeled based on 3D cylindrical coordinate. A study was performed with parameters of the location of molten drop release, break size, melting temperature, cavity water subcooling, triggering time and explosion position, so as to establish parameters' influence on the fuel-coolant interaction behavior, to determine the most challenging cases and to estimate the expected pressure loadings on the cavity walls. The most dangerous case shows the pressure loading is above the capacity of a typical reactor cavity wall.

Keywords: Steam explosion, Fuel coolant interaction, Numerical analysis, Severe accident

DOI: 10.13538/j.1001-8042/nst.25.030601

I. INTRODUCTION

Studies have been carried out for years on severe accidents in nuclear power plants (NPPs), including complicated problems of multiphase flow and heat transfer. An important issue in a severe accident is the likelihood and the consequences of a steam explosion, which may occur when the hot core meltdown comes into contact with the coolant water. When the energy of a molten corium is transferred to the coolant water in a timescale smaller than the timescale for system pressure relief, it induces dynamic loading of surrounding structures [1]. Although NPP safety analyses revealed a low probability of steam explosion occurrence as a severe reactor accident consequence, steam explosions are an issue of nuclear safety importance that may lead to a vessel's vertical displacement and challenge the containment integrity of the NPP [2–4].

As the molten drops fall into the cold liquid, hydrodynamic instabilities break up the molten jet and disperse it into the coolant to form a coarse mixture (on 1 cm scale in the case of molten corium and water). After that, film boiling occurs around the molten drops due to the large temperature difference, and the vapor film separates the molten drops from the coolant. Under some conditions, such as external pressure pulse, the vapor film collapses, allowing direct contact of the molten metal with coolant and causing further fragmentation of the molten drops. This leads to a sharp increase of the heat transfer area, evaporating the ambient liquid in a short time and generating high pressure pulse. This form of destructive instant evaporation, which can be propagated and amplified, is called steam explosion [1]. The steam explosion process is commonly divided into four phases, i.e. premixing, triggering, propagation and expansion [5].

Despite all these efforts, the nature of FCI is complex, the modeling of ex-vessel steam explosion is difficult, and the analysis results are subject to large uncertainties [6]. Examples of one- and two-dimensional FCI models include the TEXAS code [7] and the PM-ALPHA/ESPROSE computer codes [8, 9]. Additional experimental and analytical work is needed to evolve the FCI codes. In addition to the uncertainties inherent in modeling FCI processes, other uncertainties that affect the explosion energetics include the location of the melt release, the break size, the melt temperature, the cavity water subcooling, the triggering time and position for explosion calculations.

The FCI processes were modeled using the PM-ALPHA and ESPROSE computer codes [4]. PM-ALPHA is a two-dimensional computer code. JSI (Jožef Stefan Institute, Slovenia) and CEA (Atomic Energy Commission, France) developed a two dimensional geometrical model based on typical pressurized water reactor (PWR) with MC3D [10]. Simulation results of reactor vessel's failure indicate that if the failure occurs at the vessel bottom, the pressure load and impulse distribution are considerably overestimated compared to the test data from the SERENA.

It is considered that this inconsistency is caused by discrepancies between the two dimensional Cartesian geometrical model and the prototype reactor. IRSN (Institut de radioprotection et de sûreté nucléaire, France) carried out a series of ex-vessel FCI simulations with MC3D based on typical French PWR. The analysis indicates relatively a low pressure load in a long duration that may leads to wall's rupture in the reactor cavity, and a relatively high pressure in a short duration that may destroy the cavity wall, too. Also, probability of containment failure is the highest at high pressure of reactor vessel, with a large breach, or with relatively low subcooling.

In this work, aimed at predicting the consequence of ex-

* Supported by National Science and Technology Major Project of China (No. 2011ZX06004-008)
† Corresponding author, zhouyuan1911@126.com

vessel steam explosions in a typical PWR cavity, a 3D calculation model was built based on the MC3D code. Analysis was performed on different parameters of the melting release location, break size, melting temperature, cavity water subcooling, the triggering time, and position of explosion. The most challenging ex-vessel steam explosion cases were identified and analyzed.

II. MODELING

A. Introduction of the computer code

Simulations were performed with the MC3D, a 3 dimension multiphase simulation computer code developed by IRSN for nuclear safety analysis. It has two modules PREMIXING for premix phase calculation and EXPLOSION for explosion calculation. The PREMIXING module [11] describes a core-melting process by a continuous field, discontinuous field, and fuel fragment field, which correspond to melt jet, melt drop and fine fragments, respectively, in addition to other three fields of the water, vapor, and non-condensable gas. It is used for simulating the melting jet's breaking up into relatively large size drops and their fragmentation into finer drops, and the heat transfer between melting fuel rods and coolant. It has two modes of jet breakup. In one mode, the jet-breakup ratio is obtained from standard test and the molten drop size can be set by the users. In the other mode, the jet breakup rate and molten drop size are defined by the local velocity derived from Kelvin Helmholtz instability. This mode, however, is not verified sufficiently, our simulation adopted the first mode and the molten drops are sized at 4 mm.

The EXPLOSION module, in which only two fields related to the dispersed fuel are considered, is used to simulate the finer fragmentation of molten drops and heat transfer between the finer fragments and coolant. Both the thermal and hydrodynamic fragmentation processes are considered. The fragment size, defaulted at 100 μm based on the KROTOS facility test [4], can be set by the user.

It is hypothesized in MC3D that metal alloy is completely melted at temperatures beyond its melting point. However, a layer of solid shell forms before the mean temperature of a molten drop falls below the melting point, and this stops further fragmentation. Consequently, the explosion process is exaggerated in the simulation, which is conservative in the safety analysis [11].

After over 10 years of modification and development, the reliability of MC3D code has been validated in the SERENA program organized by OECD. At present, this code is of version 3.56, but in this paper we use an improved numerical method, to shorten the computing time of solving large-scale grid and enhance the stability.

B. Fragmentation model [11]

The fragmentation of molten drops is an important stage of steam explosion. The fragmentation model determines the triggering time, intensity and propagating range of the steam explosion. The mechanism used in MC3D includes thermal triggering and hydrodynamic triggering.

The code uses direct contact between the molten drop and coolant as the mechanism of thermal triggering which leads to the drop fragmentation. To fix initial time of the contact, one needs to calculate the fluid acceleration in the grid, which is proportional to the pressure difference between the coolant around the drop and the vapor film. In the non-linear Rayleigh-Taylor instable stage, the fluid acceleration (r_J) can be derived from the Taylor formula,

$$r_{\mathrm{J}} = 2(P_{\mathrm{l}} - P_{\mathrm{v}})/(\rho_{\mathrm{l}} D_{\mathrm{d}}), \tag{1}$$

where, P_{l} and P_{v} are the coolant and vapor film pressures, respectively; ρ_{l} is density of the coolant; and D_{d} is diameter of the molten drop. The fragmentation is not continuous in physical model. The discontinuity cannot be introduced into computation code while we can only take an average value in the grid. Assuming that the drop size variation and fragment rate are continuous, the initial time of fragmentation, the mass and fragment diameter can be deduced from the fragmentation model proposed [11].

Fragmentation regulation is consistent with cosine law:

$$\Gamma_{\mathrm{d}f-t} = \Gamma_{\mathrm{frag}}\{1 - \cos[2\pi/t_{\mathrm{frag}-T}]t\}/2, \tag{2}$$

where $\Gamma_{\mathrm{d}f-t}$ is the thermal fragmentation rate; Γ_{frag} is the fragmentation rate; and $t_{\mathrm{frag}-T}$ is the fragmentation time. The largest fragmentation rate is:

$$\Gamma_{\mathrm{frag}} = 2m_{\mathrm{frag}}/t_{\mathrm{frag}-T}, \tag{3}$$

where m_{frag} is mass of the fragmentation. The other triggering mechanism is hydrodynamic triggering. After explosion, the fluids are accelerated from their initial velocity by the pressure impact, and large enough velocity differences may lead to fragmentation. So, the fragmentation caused by the hydrodynamic triggering is dominant. This can be attributed to the peel off of hydraulic boundary layer of the coolant fluid formed outside the molten drops or the Rayleigh-Taylor instability caused by acceleration of the coolant of a smaller density near the drop.

At present, MC3D applies the peel off mechanism. The fragmentation rate is

$$\Gamma_{\mathrm{d}f-h} = \alpha_{\mathrm{d}} \Delta V_{\mathrm{dc}} (\rho_{\mathrm{d}} \rho_{\mathrm{c}})^{1/2} / (t^*_{\mathrm{frag}} D_{\mathrm{d}}), \tag{4}$$

where, $\Gamma_{\mathrm{d}f-h}$ is the hydrodynamic fragmentation rate, α_{d} is volume fraction of the molten drops, ΔV_{dc} is relative velocity between the continuous phase and molten drop, ρ_{d} is density of the molten drops, ρ_{c} is density of the coolant, t^*_{frag} is characteristic time, and D_{d} is diameter of the molten drops, And $t^*_{\mathrm{frag}} = 1$ is recommended (it varies from 1 to 1. 25).

C. Geometrical model and initialization

1. *Geometrical model and grid generated*

The geometrical model used in this paper is based on 1000 MW PWR. However, the MC3D simulation would take too much time if all the complex NPP structures are modeled. So, only the structures that affect the FCI process are taken into consideration.

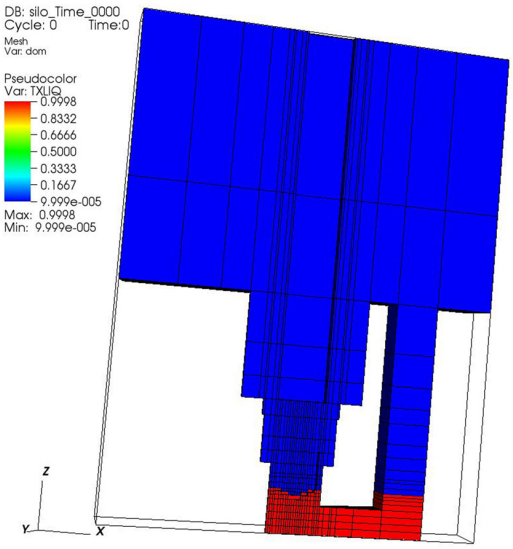

Fig. 1. (Color online) Geometry of 3D model of nuclear island structures.

The nuclear island modeled in this paper mainly focuses on the reactor cavity and venting tunnel. Only half of the structures are analyzed because of symmetry. As shown in Fig. 1, the red part below the reactor pressure vessel stands for the coolant water in the cavity and venting tunnel. The numerical grid is adequately refined in this part, which is important for simulating the FCI process.

In Table 1, a numerical grid in cylindrical coordinate is given. Each mesh is represented by its coordinate (γ, θ, z) number. Since only half of the structure is analyzed, just four θ values (0, $\pi/12$, $11\pi/12$ and π) are needed, while there are 20 nodes on the γ axis and 22 nodes on the z axis.

In sensitivity analysis, the location (8, 1, 9) and (11, 3, 3) are chosen (Fig. 2) as reference locations in the bottom of pressure vessel and the cavity wall, respectively. The pressures at the two locations are recorded.

2. *Initial conditions*

An assumed accident of pressure vessel failure developed from large break LOCA is used as the standard case. The initial conditions are set reasonably to expected conditions at vessel failure. All sensitivity analyses later are deduced from comparison to the standard case. Table 2 shows initial conditions of the standard case.

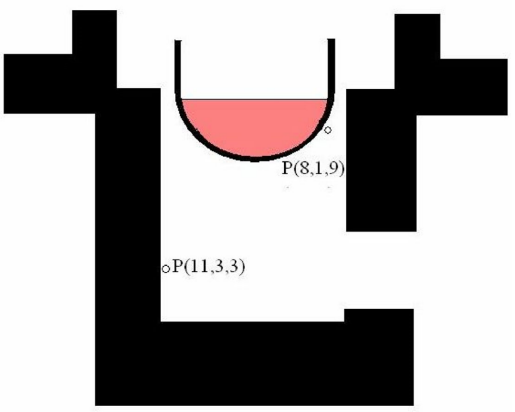

Fig. 2. (Color online) The reference locations in the bottom of pressure vessel and the cavity wall.

III. SIMULATION AND ANALYSIS

A. Simulation results of standard case

1. *Variation of volume fraction distribution*

The simulation results obtained in both the premixing and explosion processes include temperature field, pressure field and volume fraction field. The volume fraction distributions in the premixing and explosion processes, after the pressure vessel failure and the melting, are shown in Figs. 3 and 4. The thermal interaction of the melting rods with the coolant is much more violent in the explosion process than that in the premixing process. So most corium in cavity remains below the location where the failure hole exists during the premixing process, while the corium disperses and spreads out in the explosion process.

2. *Variation of the pressure field*

Figure 5 shows the pressure field variation in the premixing process of the standard case. It decreases slowly in the premixing process, without obvious pressure pulses. Fig. 6 shows the pressure field variation in the explosion process of the standard case. From the comparison of Fig. 5 and Fig. 6, the pressure increases to a high level rapidly after the triggering of the explosion, which dissipates slowly. The pressure field distributes non-uniformly in the cavity and varies rapidly. The explosion lasts for just 0.05 s, much shorter than the premixing process.

B. Pressures of the reference locations in the explosion process

1. *Pressures at different locations in the circumferential direction*

Figure 7 shows the pressures for different locations at the bottom of the pressure vessel and on the cavity wall, at

TABLE 1. The coordinate (γ, θ, z) number and values used in the MC3D simulation.

No.	1	2	3	4	5	6	7	8	9	10	11	12	13	14	15	16	17	18	19	20	21	22
γ/m	0	0.25	0.45	0.65	0.85	1.12	.135	1.62	1.99	2.18	2.43	2.64	3.06	3.69	3.90	4.38	6.12	9.07	13.34	19.04	–	–
θ/π	0	1/12	11/12	1	–	–	–	–	–	–	–	–	–	–	–	–	–	–	–	–	–	–
z/m	0	0.77	1.45	2.13	2.82	3.39	3.81	4.14	4.44	4.99	5.55	5.90	6.86	8.11	9.43	11.50	13.07	15.25	18.52	23.52	33.54	50.00

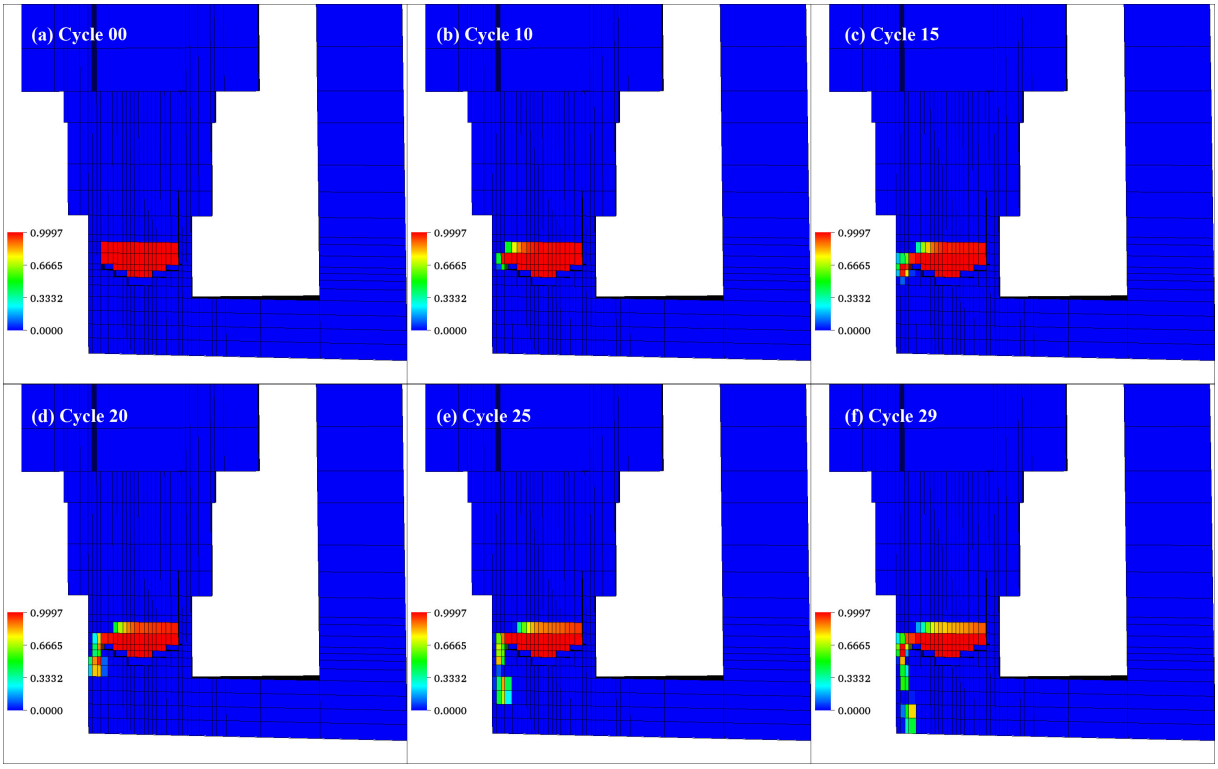

Fig. 3. (Color online) Volume fraction distribution in the premixing process of the standard case.

TABLE 2. Initial parameters in the standard case.

Initial conditions	
Melt temperature (K)	2650
Melt level (m)	1.73
Gas temperature in PV (K)	720
PV pressure (Pa)	287000
Gas temperature in containment (K)	396
Containment Pressure (Pa)	287554
Mole fraction of vapor	0.605
Mole fraction of hydrogen	0.018
Break size (m)	0.4
Melt release angle (degree)	85
Coolant subcooling (K)	0
Water level (m)	4. 3
Triggering time (s)	2.0
Triggering position	(9, 3, 3)

different θ values, in the explosion process of the standard case. The locations chosen for analysis at the pressure vessel bottom (Fig. 7(a)) are (8, 1, 9), (8, 2, 9) and (8, 3, 9), and on the cavity wall are (11, 2, 11) and (11, 3, 11). One sees that the pressure curves of different locations are almost overlapped. So the change of θ has little effect on the pressure variation at the pressure vessel bottom.

2. *Pressures at different locations in the radial direction*

Figure 8 shows the pressures at different locations in the pressure vessel bottom and on cavity wall in the radial direction in the standard case.

The locations chosen for analysis are (3, 3, 6), (5, 3, 7) and (8, 3, 9) in the pressure vessel bottom (Fig. 8(a)), and (11, 3, 1), (11, 3, 3) and (11, 3, 11) on the cavity wall (Fig. 8(b)). One sees that the pressures rise rapidly after triggering, and the maximum pressures are over 100 bar in Fig. 8(a) and over 500 bar in Fig. 8(b). Within 0.02 s, the pressures decrease rapidly towards the original level. The pressure variation in γ coordinate is not significant. In Fig. 8(b), pressure oscillations are seen, and the oscillation amplitude decreases with increasing distance from the triggering location.

Figure 9(a) shows pressures versus height of the cavity wall at 0–5 seconds in the premixing process. The maximum pressure, occurring at about 1 s, locates at the cavity floor and decreases linearly with increasing height towards a constant

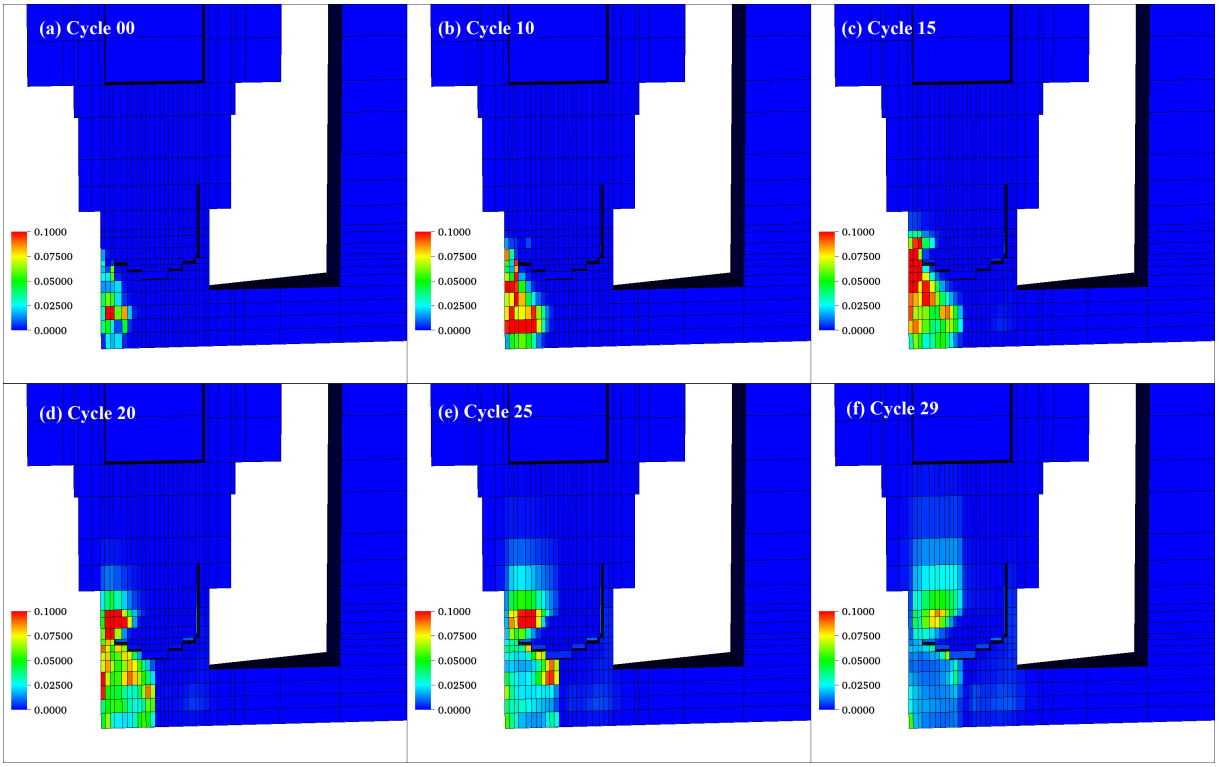

Fig. 4. (Color online) Volume fraction distribution in the explosion process of the standard case.

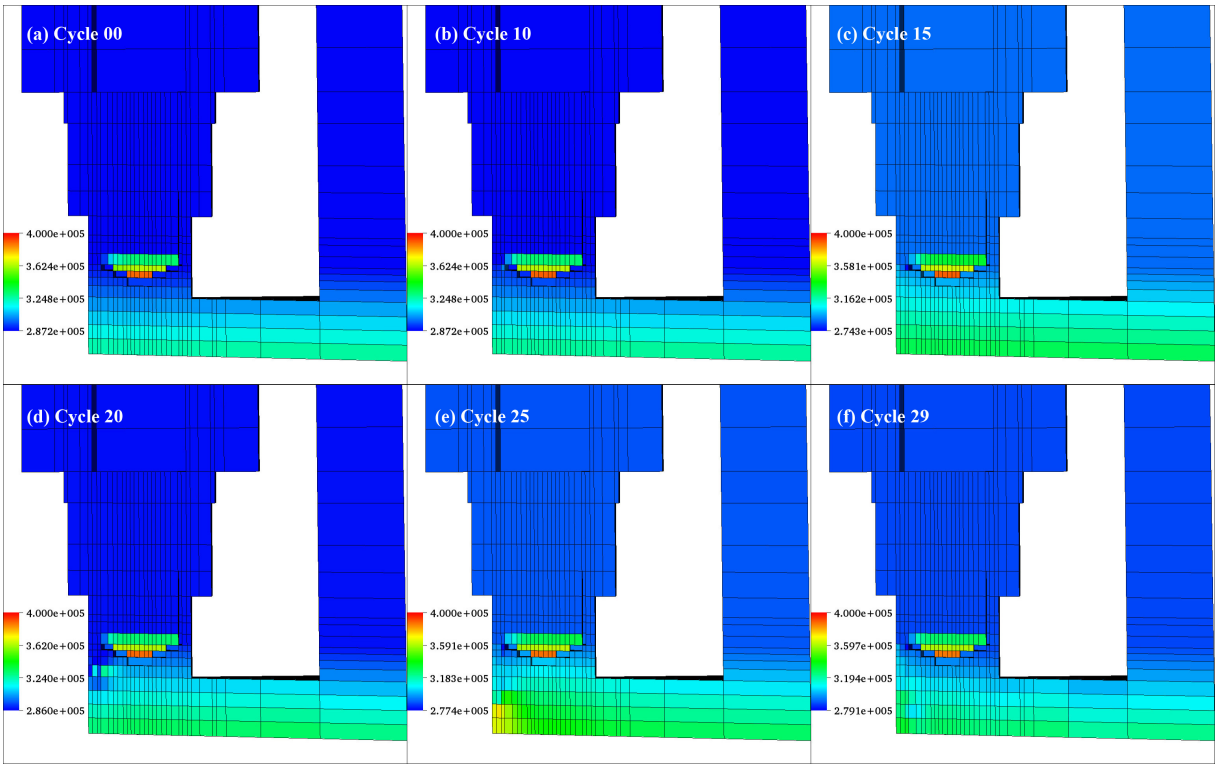

Fig. 5. (Color online)Variation of the pressure field in the premixing process of the standard case.

at the cooling water level. The pressures on the cavity wall in the explosion process are shown in Fig. 9(b). The maxi-

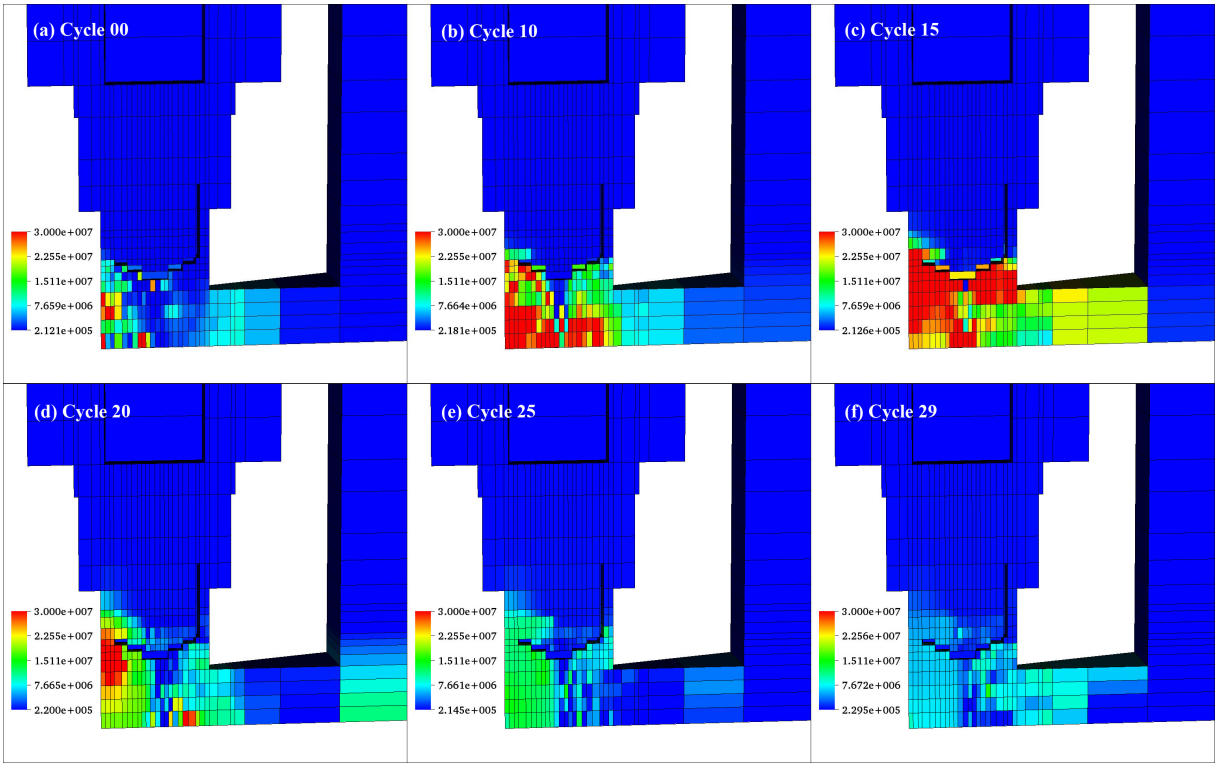

Fig. 6. (Color online) Variation of the pressure field in the explosion process of the standard case.

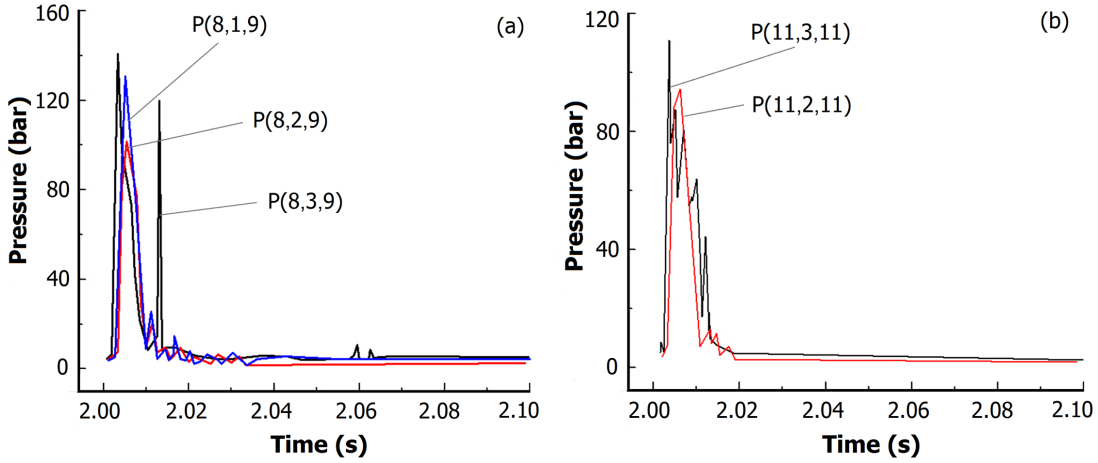

Fig. 7. (Color online) Pressures at different locations in the pressure vessel bottom (a) and on the cavity wall (b), in the circumferential direction.

mum pressure on the cavity wall is reached about 0.002 s after the triggering. The pressure decreases with increasing height, and the explosion dissipates slowly after 0.015 s. The explosion affects the pressures on the wall below the coolant water level, while the pressures above the cooling water changes little during the explosion.

C. Detailed analysis

1. *Sensitivity analysis of pressure vessel failure location*

Figure 10 shows the peak pressures and pressure loadings at the reference locations of (8, 1, 9) and (11, 3, 3) in the explosion process as function of the melting release angle, i.e. location variation of the pressure vessel failure. The pressure loadings are calculated with an integration period of 0.1 s af-

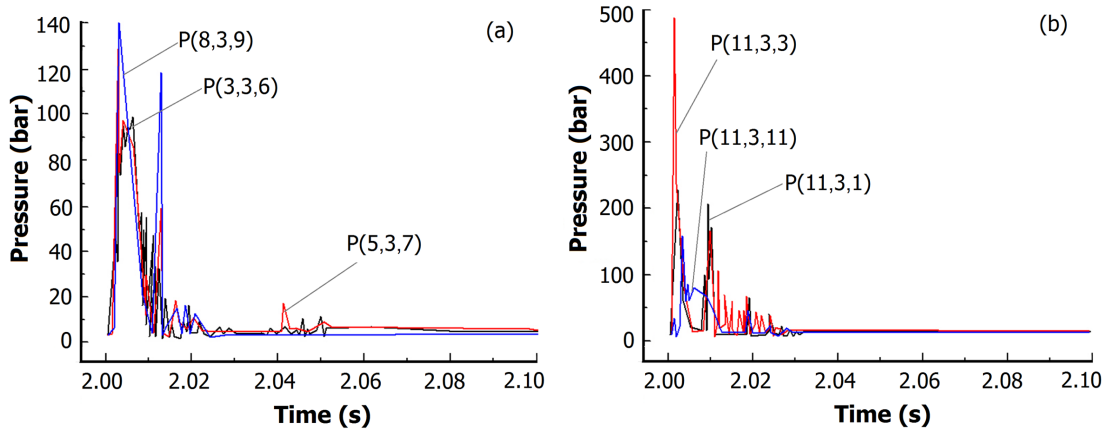

Fig. 8. (Color online) Pressures at different locations in the pressure vessel bottom (a) and on the cavity wall in the radial direction.

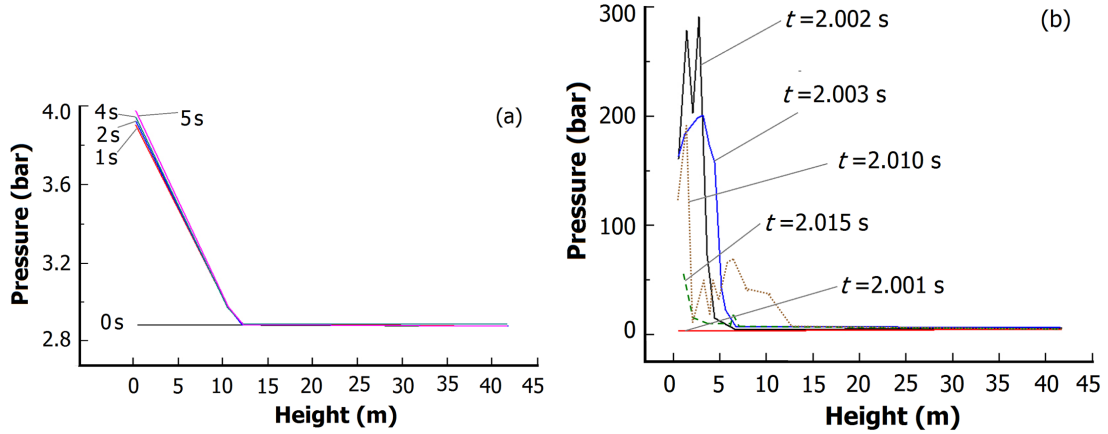

Fig. 9. (Color online) Pressures at the locations of different heights on the cavity wall in the premixing (a) and explosion (b) processes.

ter the triggering.

In Fig. 10, the highest pressure and pressure loadings for both locations occur when the pressure vessel failure is located where the melting release angle is 50° in the bottom of vessel. The pressure and pressure loadings at the pressure vessel bottom is relatively small and the pressure on the cavity wall is high at the release angle of 85°.

2. *Sensitivity analysis of size of the pressure vessel failure*

Figure 11 shows the peak pressures and pressure loadings for the reference locations of (8, 1, 9) and (11, 3, 3) as function of the pressure vessel failure size (from 0.1 m to 0.8 m) in the explosion process. The pressure loadings are calculated with an integration period of 0.1 s after the triggering. Generally, the peak pressure and pressure loadings increase with the size of pressue vessel failure. In Fig. 11(b), the highest pressure loading occurs at 0.7 m of the failure diameter. Since more corium flows out when the failure size becomes larger, the capacity to cause violent interactions grows up correspondingly, though it does not increase all the way.

3. *Sensitivity analysis of the coolant temperature*

For different scenarios, the coolant water temperature is different, but it varies certainly from the room temperature to the saturation temperature at the corresponding pressure. The coolant temperatures of 300 K, 320 K, 340 K, 345 K, 350 K, 355 K, 360 K, 378 K and 396 K are used to analyze the coolant temperature effect on the FCI process. Fig. 12 shows the pressure peaks and pressure loadings (in an integration period of 0.1 s after the triggering) at the reference locations of (8, 1, 9) and (11, 3, 3) at the above coolant water temperatures.

In Fig. 12(a), the peak pressure increases with the coolant temperature on the cavity wall, while it increases at first in the pressure vessel bottom but decreases at the coolant temperatures higher than 340 K. In Fig. 12(b), the pressure loading maximized at 345 K of the coolant water temperature. Higher coolant temperature means higher metal temperature and vapor volume. High metal temperature cause violent interaction and high pressure, but large vapor volume fraction leads to explosion suppression. This means that the pressure loading is small at coolant water temperatures being much smaller than

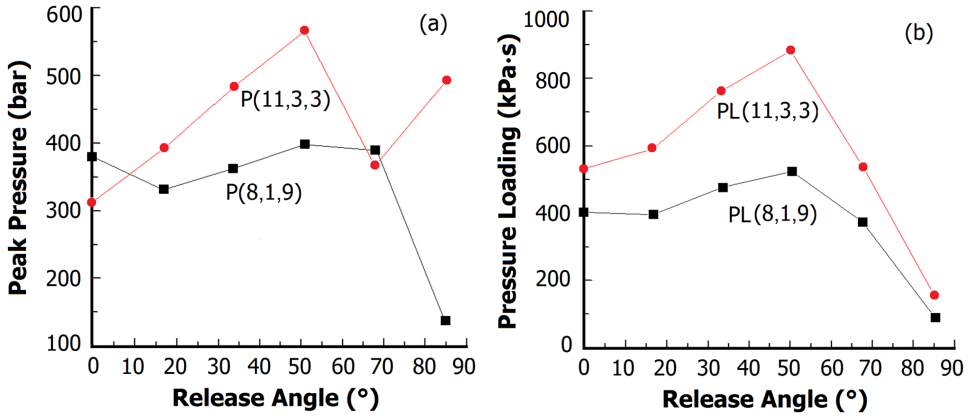

Fig. 10. (Color online) Peak pressures (a) and presuure loadings (b) at reference locations (8, 1, 9) and (11, 3, 3) as function of the melting release angle.

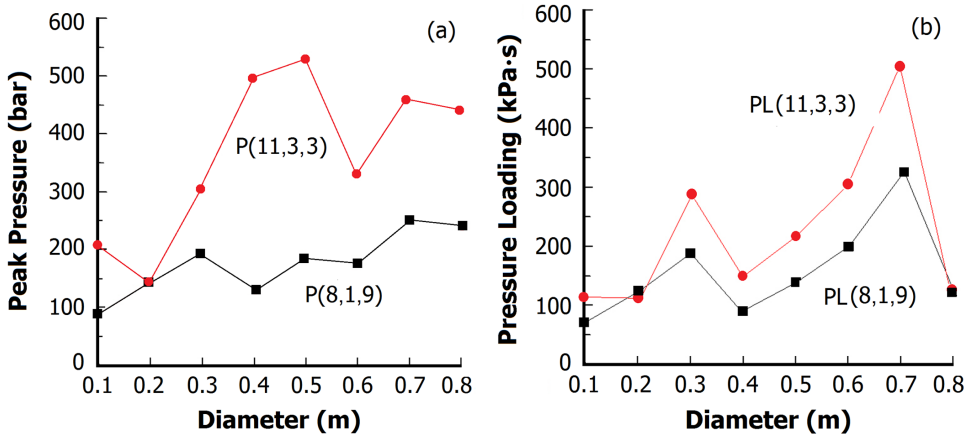

Fig. 11. (Color online) Peak pressures (a) and presuure loadings (b) at locations (8, 1, 9) and (11, 3, 3) as function of pressure vessel failure size.

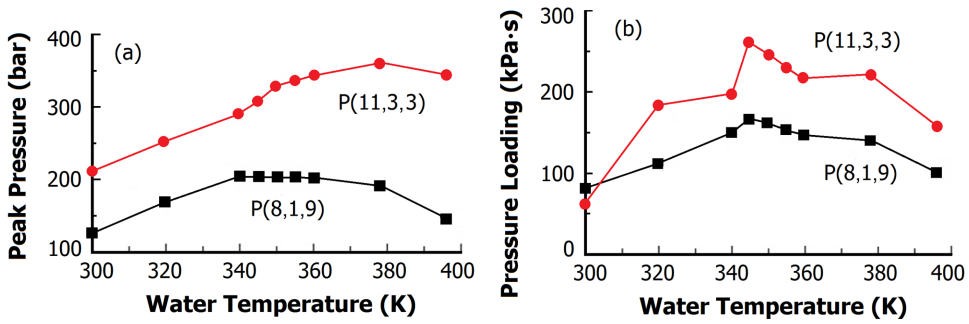

Fig. 12. (Color online) Peak pressures (a) and presuure loadings (b) at locations (8, 1, 9) and (11, 3, 3) as function of the coolant water temperature.

or close to the saturation temperature.

4. *Sensitivity analysis of melting temperature*

It can be seen that the peak pressures at the location (11, 3, 3) (the cavity wall) are about 500 bar (and may remain in the high value at even higher fuel temperatues), while the peak pressures at location (8, 1, 9) (the pressure vessel bot-

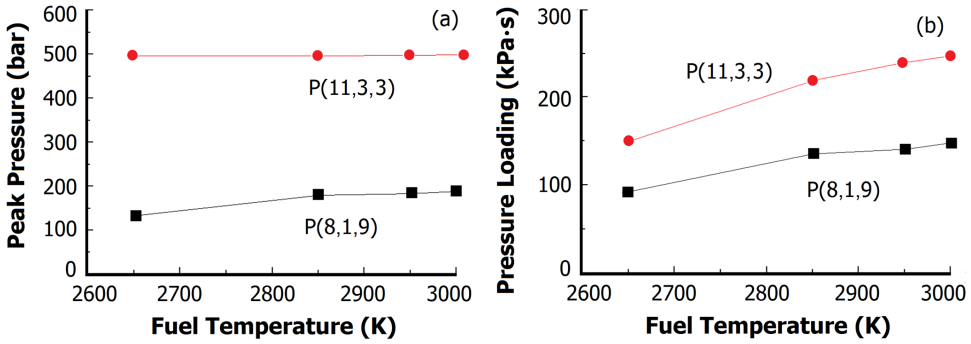

Fig. 13. (Color online) Peak pressures (a) and presuure loadings (b) at locations (8, 1, 9) and (11, 3, 3) as function of the melting temperatures.

tom) increase slightly with melting temperature (Fig. 13(a)); and the pressure loadings (calculated with an integration period of 0.1 s after the triggering) of both locations increase with the temperature (Fig. 13(b)). The melting temperature induces more rapid heat transfer and the steam explosion becomes stronger.

5. *Sensitivity analysis of triggering time*

In the previous calculations, the time t is 2.0 s after the FCI process. So, the triggering time effect on the FCI process is analyzed at t =1.40, 1.55, 1.70, 1.85, 1.90, 2.00, 2.10 and 2.20. As shown in Fig. 14(a), the peak pressures at the location (11, 3, 3) increases first but begin to decrease at 1.7 s. The peak pressure at location (8, 1, 9) varies slightly with the triggering time. As is shown in Fig. 14(b), calculated with an integration period of 0.1 s after the triggering, the pressure loadings of both locations increase first but decrease after 1.7 s. With a greater triggering time, the molten metal mass increases, causing more violent interaction. However, with the delayed triggering time, the molten drops interact longer with coolant water and generate more vapor. The volume fraction of vapor increases and the volume fraction of coolant water decreases correspondingly. Therefore, the transfer area between the molten drops and water decreases and less vapor are generated after triggering time, the pressure peak and pressure loadings decrease at last.

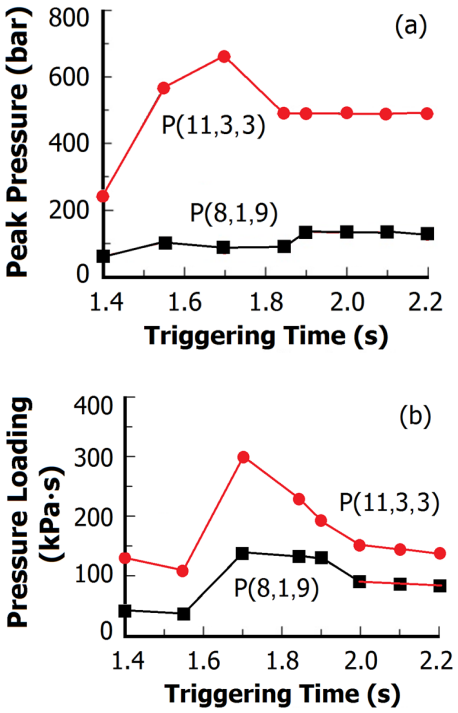

Fig. 14. (Color online) Pressure peaks for different triggering time.

6. *Sensitivity analysis of triggering position*

The triggering positions, according to the previous computation, are at the interaction zone close to the cavity floor. The triggering position effect on the FCI process is analyzed at the heights of 2.13 m, 2.82 m and 3.39 m. Table 3 shows the results. The peak pressures at the location (11, 3, 3) decreases with increasing height of the triggering position. As the triggering positions are far away from the location (8, 1, 9), so the changes in triggering position do not affect the peak pressure. For both locations, the pressure loadings, calculated with an integration period of 0.1 s after the triggering, increase slightly with the height of triggering position. The triggering position does not affect the FCI process obviously.

TABLE 3. Peak pressures and pressure loadings of reference locations (8, 1, 9) and (11, 3, 3) at different triggering positions (the cavity wall height) in the explosion process

Height (m)	Peak pressure (bar)		Pressure loading (kbar.s)	
	(8, 1, 9)	(11, 3, 3)	(8, 1, 9)	(11, 3, 3)
2.13	130	495	90	150
2.82	127	325	94	152
3.39	122	220	100	155

TABLE 4. Initial parameters in the standard case.

Initial conditions	
Melt temperature(K)	3000
Size of the pressure vessel failure (m)	0. 8
Melt release angle(degree)	45
Coolant temperature(K)	345
Triggering time(s)	1. 7
Triggering position	(9, 3, 3)

D. The most dangerous case

From the sensitivity analysis, the pressure vessel failure size has a greater effect on the interaction. The assumed accident is that the vessel fails around nearly all its circumference. In this situation, plenty of the molten drops go into the coolant water in a short time. The initial condition of the most dangerous case is given in Table 4. The coolant water temperature is set as 320 K, at which both the peak pressure and pressure loading reach their maximum. And other parameters are given based on the analysis results above.

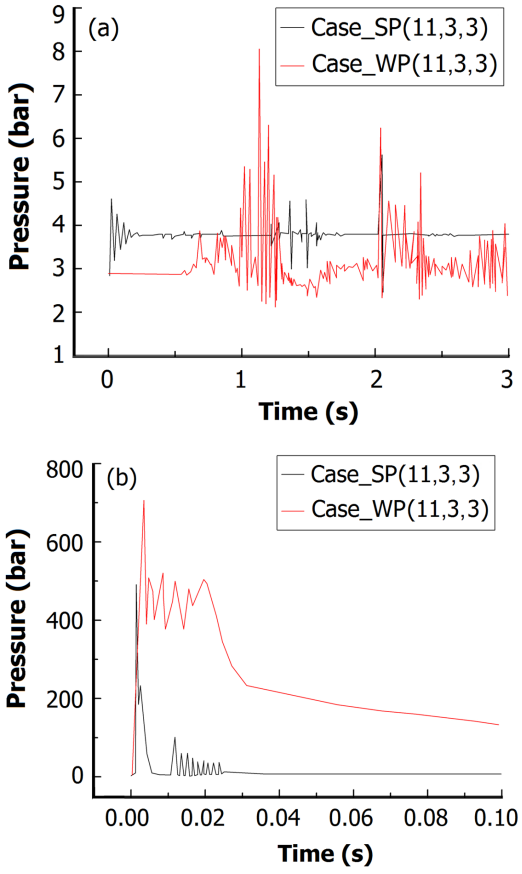

Fig. 15. (Color online) Pressures in the premixing (a) and explosion (b) processes for the most dangerous (Case_WP) and standard (Case_SP) cases.

Figure 15 shows the pressures at the location (11, 3, 3) in the premixing and explosion processes for the most dangerous case (labeled as Case_WP) and the standard case (labeled as Case_SP). The location close to the cavity floor is analyzed. In Fig. 15(a), the pressure variation for the most dangerous case is much more violent than the pressure variation for the standard case, with the pressure peak of about 8 bar. In Fig. 15(b), the pressures of both the cases increase sharply to a peak at first. Then, the pressure of the standard case decreases rapidly, while the pressure of the most dangerous case remains at a pretty high level for about 20 ms before it begins to decrease slowly. So the pressure loading for the most dangerous case is much higher and may endanger the surrounding structures and challenge the containment integrity.

IV. CONCLUSION

An assessment of ex-vessel steam explosion pressure loads in a typical pressurized water reactor cavity was performed with the code MC3D. In order to assure that the calculation results reflect qualitatively and quantitatively the complex geometry effect of a real reactor cavity, a 3D cylindrical coordinate model is developed to perform a series of simulations. A parametric analysis has been performed to establish the influence and importance of different parameters on the FCI outcome and to eventually capture the most severe steam explosions.

The assumed accident of pressure vessel failure which developed from large break LOCA (LBLOCA) is selected as the standard case. The initial conditions are set reasonably to expected conditions at vessel failure. The pressures and corresponding pressure loadings of different locations in the pressure vessel cavity are calculated in this paper. It suggests that the pressure changes little with the location variations at the bottom of the pressure vessel in the circumferential direction, in the radial direction and on the cavity wall in the circumferential direction. The pressure peaks on the cavity wall decrease with height increase. The explosion affects the pressures below the surface of the coolant water mainly, while the pressures on the cavity wall above the water changes little during the explosion process. The triggering position is at the bottom of the cavity and the pressure is higher at the location where it is closer to the triggering position.

The calculation results suggest that the most challenging situation occurs when the PV failure locates at the place where the melt release angle is 45°. The flow rate of the melt increases when the size of the PV failure becomes larger, and stronger explosion would occur. The pressure loading increases first and decreases when the triggering time is delayed. With the delay of the triggering time, metal mass increases which lead to more violent interaction. However metal temperature decreases and more vapor is generated. The volume fraction of vapor increases, which makes the pressure loadings decrease at last. The variation of the triggering position has little effect on the FCI process.

In the presented study a number of simulations were performed, systematically searching for the strongest explosions in the considered conditions, whereas in Matjaz Leskovar and

Mitja Ursic study, there were only three melt release location conditions and the effects of water level and triggering position were not mentioned. In SERENA project only one central melt pour scenario was analyzed. In this paper the most dangerous scenario is obtained after considering all the sensitivity analysis results. It suggested that the pressure peak for the most dangerous case may reach 700 bar and remains at a pretty high level for a long time and the pressure loading is far over 0.1 MPa s. It may result in the failure of the cavity structure at last. The process of FCI is so complex that small model changes in the process can have a significant influence on the simulation results. Therefore additional experimental and analytical work is needed to validate the computer code in the future.

[1] Berthoud G. Annu Rev Fluid Mech, 2000, **32**: 573–611.
[2] Theofanous T G. Nucl Eng Des, 1995, **155**: 1–26.
[3] Almstroem H, Sundel T, Frid W, *et al*. Nucl Eng Des, 1999, **189**: 405–422
[4] Esmaili H and Khatib-Rahbar M. Nucl Eng Des, 2005, **235**: 1583–1605.
[5] Corradini M L, Kim B J, Oh M D. Prog Nucl Energ, 1988, **22**: 1–117.
[6] Meigen R. Proceedings of ICAPP'05, Seoul, Korea, 2005, pp. 411–423.
[7] Young M F. The TEXAS code for fuel-coolant interaction analysis. Proceedings of ANS/ENS LMFBR Safety Topical Meeting, Lyon-Ecully, France, 1982.
[8] Yuen W W and Theofanous T G. PM-ALPHA: a computer code for addressing the premixing of steam explosions. DOE/ID-10502, 1995.
[9] Theofanous T G and Yuen W W. ESPROSE. m: A computer code for addressing the escalation/propagation of steam explosions, DOE/ID-10501, 1995.
[10] Leskovar M and Uršič M. Nucl Eng Des, 2009, **239**: 2444–2458.
[11] Meignen R. Description of the physical models of the explosion application. France: IRSN, 2008.